Powering 3 Dimensional Microrobots: Power Density Limitations *

Ronald S. Fearing
Department of EE&CS
University of California
Berkeley, CA 94720-7440
September 27, 1998

Abstract

Many types of electrostatic and electromagnetic microactuators have been developed. It is important to understand the fundamental performance limitations of these actuators for use in micro-robotic systems. The most important consideration for micro mobile robots is the effective power density of the actuator. As inertia and gravitional forces become less significant for small robots, typical metrics for macro-robots, such as torque-to-weight ratio, are not appropriate. A very significant problem with micro-actuators for robotics is the need for efficient transmissions to obtain large forces and torques at low speeds from inherently high speed low force actuators.

1 Introduction

Many varieties of micro-actuators based on electrostatic and electomagnetic principles have been developed. This paper examines limitations of actuator force, speed and stroke, and compares representative examples of current micro-actuators. Electrostatic actuators have been simpler to fabricate, but have limited energy density compared to magnetic actuators. Piezo-electric actuators have orders of magnitude more force than electrostatic actuators due to the higher dielectric constant, but have limited strain. An important consideration for selecting actuators for micro-robots is the use of mechanical transformers such as wobble motors and inch worm drives which provide larger forces or displacements at lower speed.

For a very good introduction to the size scaling issues of magnetic and electric actuators, the paper by Trimmer and Jebens [1989] is recommended. A good survey of fully or partly IC-processed actuators can be found in Fujita and Gabriel [1991]. For a good general survey including thermal and chemical actuators, see [Dario et al 1992]. This survey considers two groups: electric field driven and magnetic field driven actuators.

For macro-scale applications, magnetic actuators are dominant. It is not clear yet which technology will be dominant at the micro-scale. One scaling law that is helpful for micro-actuators is the increased break down field strength of very small gaps due to the Paschen effect. Thus for small sizes, the obtainable electrostatic forces can be stronger than electromagnetic forces [Trimmer and Jebens, 1989]. Since electrostatic devices can be constructed using only conductors and insulators, they can be made compatible with silicon micromachining techniques. However, recent improvements in materials processing now allow deposition of thin-film magnetic materials, so integrated micro-magnetics are now possible.

For micro-robotics applications, it seems that ideal actuators would have reasonable speed, long strokes, and high force (high torque). However, many of the available actuation principles such as piezoelectric effect and electrostatic actuators tend to have a very short stroke, but high resonant frequency. Methods such as used in the ultrasonic motor and harmonic micromotor provide, in effect, a gear reduction which increases available torque.

1.1 Power Requirements for Tasks

As motivation for study of actuator scaling, let's consider example micro robot tasks: pick and place assembly, material removal (machining), and mobile robot swimming and flying.

1.1.1 Power for pick and place

A simple pick and place robot system is shown in Figure 1. To keep task completion time constant as the robot size l decreases while the workspace size L remains the same, then the acceleration $\ddot{x}$ should be

*This work was funded in part by: NSF-PYI grant IRI-9157051.

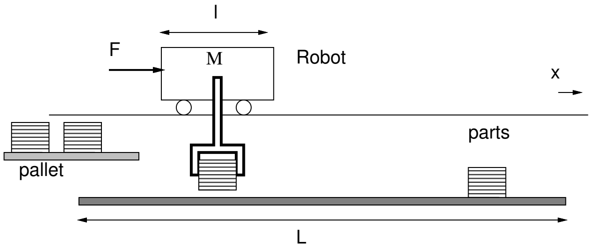

Figure 1: One dimensional pick and place robot model.

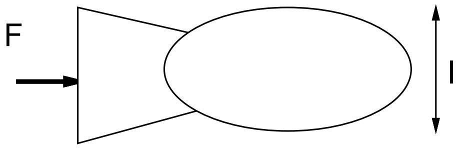

Figure 2: Simple swimming robot model.

independent of size. Since mass $M = \rho l^3$, the actuator force needs to be proportional to volume to maintain the same performance. The robot power density $\frac{P}{l^3} = \frac{F\dot{x}}{l^3}$ must also be independent of size to maintain the same performance. Of course, if the work space dimension L also scales with robot dimension, higher performance could be obtained for the smaller system.

1.1.2 Power for material removal

For a micro-robot to modify material shape such as by cutting or milling metal takes cutting enery of $4 \times 10^3 Jcm^{-3}$ [Nieble et al 89]. A conventional AC motor has power density of $200Wkg^{-1}$ or approximately $5 \times 10^5 Wm^{-3}$. Thus each cm^3 of actuator removes $0.1mm^3 sec^{-1}$ of metal. Microrobot motors typically have much less than this power density, so machining operations could be much slower at the micro-scale.

1.1.3 Power for swimming, running and flying micro-vehicles

Power for locomotion is predominantly drag limited at the microscale as inertial and gravitational forces become insignificant. For a swimming vehicle with laminar flow:

$$P_{drag} = F \cdot v = 6\pi r \mu v^2, \tag{1}$$

where μ is the viscosity of water. If velocity and size are proportional to l, then P_{drag} is proportional to l^3. With $l = 1cm$ and velocity $v < 0.2ms^{-1}$ (laminar flow) $P_{drag} \approx 10^{-5}W$, or $20Wm^{-3}$, a very small power density requirement.

For a legged micro-robot (following [Shimoyama 1991, 1995]) with walking velocity of $5mms^{-1}$, the

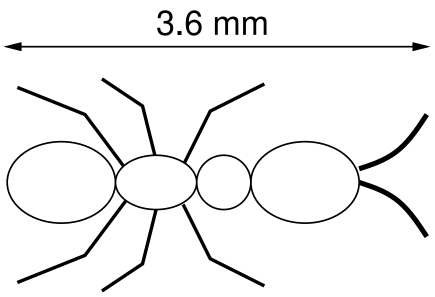

Figure 3: Ant-like micro-robot.

required joint torque is $5 \times 10^{-9} Nm$ and joint velocity $10rads^{-1}$. Thus the average power for 3 legs with 3 DOF each is $5 \times 10^{-7}W$ or $2 \times 10^3 Wm^{-3}$. The required static torque is a product of leg length and body weight, so required torque scales as l^4. The joint velocity scales as $l^{\frac{-1}{2}}$, thus the required power density $\frac{P}{V}$ is proportional to $\sqrt{l}$. Hence smaller robots require lower power density for appropriate scale speed.

For a flying micro-vehicle, following [Shimoyama 1995], the drag force on the wings is:

$$F_D = C_D \tfrac{1}{2} \rho U^2 A \ , \tag{2}$$

where C_D, ρ, U, A are the drag coefficient, air density, relative air velocity, and wing area, respectively. This drag force needs to balance the weight $F_g = mg$ of the robot. With U proportional to $\sqrt{l}$, the required power is $P = F_D U$ which is proprtional to $L^{\frac{7}{2}}$, and power density $\frac{P}{V}$ is proportional to $\sqrt{l}$. Thus, the required power density is favorable for small flying robots.

1.1.4 Power density for microactuators

As seen above, a constant power density with scale is required for high performance micro-robot pick-and-place, walking and flying micro-robots. As this survey shows, most current micro-actuators are far removed from the power density achieved by macro size actuators.

2 Electric Field Driven Actuators

There are a variety of electric field driven actuators, based on principles of electrostatic attraction, piezoelectricity, or quasi-static induction. Many types of micro-actuators have been designed, both linear and rotary, using tangential drive and normal drive.

Small tools impractical to fabricate by other methods, for example, an electrostatically driven gripper able to handle 10 μm diameter parts [Kim et al, 1992], can be made by surface and bulk micromachining of silicon. Among the many other novel devices made possible, are planar rotary micro motors [Fan et al, 1989], Trimmer and Gabriel [1987] and dielectric induction motors [Fuhr et al 1992a, 1992b]. The drawback to these devices, even with small gaps, is the low force and torque obtainable. The gripper built by Kim has a grasping force on the order of $1\mu N$, while the electrostatic micromotor has a diameter of 100 μm and torque of about $10pNm$ which may be much too small for micro-robotic applications. Friction is also a problem in the rotary micromotors. Possible ways to build improved rotary actuators with higher torque are to use a vibration-to-rotation conversion [Lee and Pisano, 1991], or a harmonic micromotor [Price, Wood, Jacobsen, 1989], [Furuhata et al 1993], which can achieve torques on the order of $10\mu Nm$ with a 1 mm radius motor.

For many micro-robot applications a linear actuator may be more useful than a rotary one. Recently, integrated force arrays have been described (Bobbio et al [1993], [Kornbluh et al 1991] and Yamaguchi et al [1993]), which take advantage of the very strong normal attractive force between two parallel charged surfaces. Another type of planar mechanism, an electrostatic surface drive is described by Egawa et al [1991] and Niino, Egawa, Higuchi [1993].

Multi DOF actuators can also be driven electrostatically. Fukuda and Tanaka [1990] describe a 3 DOF actuator made using copper foil, and Wood, Jacobsen, and Grace [1987] controlled the position of an optical fiber driven electrostatically. In an important innovation, Shimoyama et al [1991], Suzuki et al [1992] have developed electrostatic actuators fabricated from polysilicon and polyimide which can act out of the plane of the wafer and have multiple degrees of freedom. These actuators are being developed to emulate insect wing joints and muscles.

2.1 Linear Electrostatic Actuators

Figure 4 shows the basic geometry of the parallel plate capacitor which is at the heart of most tangential and normal drive electrostatic actuators. (Even for the induced charge actuators, the parallel plate capacitor model provides an upper bound estimate of the available force). With a potential V applied across the top and bottom plates, the stored energy in the capacitor is given by:

$$W = \frac{1}{2}CV^2, \tag{3}$$

where the capacitance C (neglecting fringing fields) is

$$C(z) = \epsilon\frac{L_x L_y}{z} \tag{4}$$

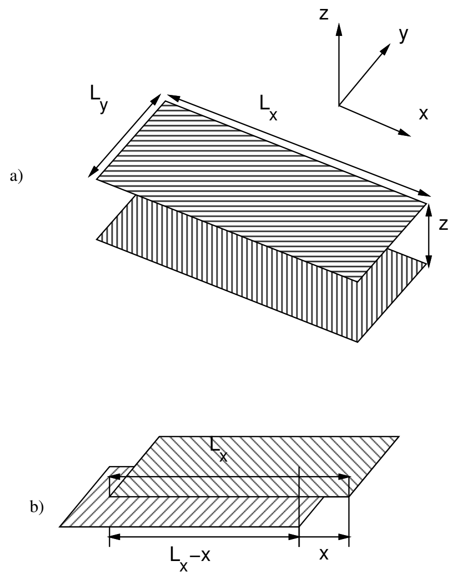

Figure 4: Parallel plate capacitor geometry. a) normal drive b) tangential drive

with z, ϵ, L_x and L_y the plate separation, permittivity, and plate dimensions respectively.

2.1.1 Normal Force Actuators

The force in the normal direction is given by:

$$F_z(z) = -\frac{\partial W}{\partial z} = \frac{1}{2}\epsilon\frac{L_x L_y}{z^2}V^2. \tag{5}$$

The equivalent "electrostatic pressure" is calculated by the normal force per area or:

$$P_{electrostatic} = \frac{F_z}{L_x L_y} = \frac{1}{2}\epsilon|E|^2. \tag{6}$$

Figure 5 shows a typical technique for building a normal drive electrostatic actuator on a planar substrate. Multiple sections can be ganged together to increase the effective area, and the actuator is bidirectional. Typically, about two thirds of the actuator is taken up by structural materials. Note that to obtain high fields and large forces, the stroke for the actuator will be very small, typically around $2\mu m$. One approach to getting substantial forces and large stroke from a parallel plate type actuator uses a sandwich of layers with a compliant suspension as shown in Figure 6. Although the peak strain of the actuator is typically less than 30%, the stack could in principle be made substantially thick.

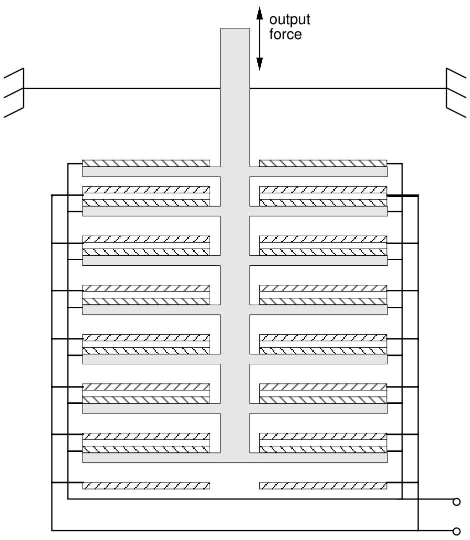

Figure 5: Parallel plate comb drive actuator.

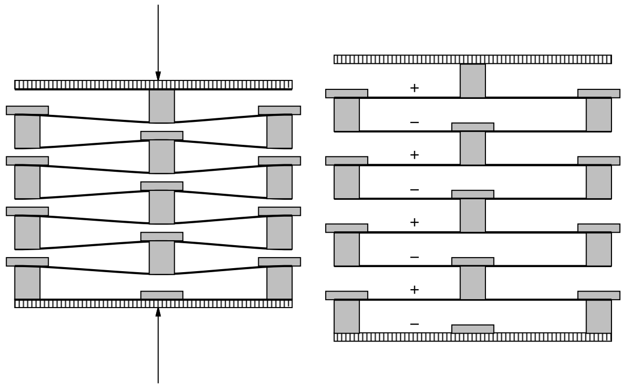

Figure 6: Integrated Force Array similar to Bobbio et al [1993]. Actuator is unidirectional, with maximum stroke of about 30%.

2.1.2 Tangential Force Actuators

For a tangential drive actuator (which requires a strong bearing to resist the F_z force, or balanced top and bottom drive), the capacitance can be written

$$C(x) \;=\; \epsilon \frac{(L_x - x)L_y}{z} \tag{7}$$

and thus the force in the tangential direction is:

$$F_x(x) \;=\; -\frac{\partial W}{\partial x} \;=\; \frac{1}{2}\epsilon \frac{L_y}{z} V^2. \tag{8}$$

Note that (again neglecting fringing fields) the tangential force is independent of the length of the plate L_x. Thus the tangential force can be increased by having many narrow plates of width L_y connected in parallel. A typical side drive actuator is shown in Figure 7,

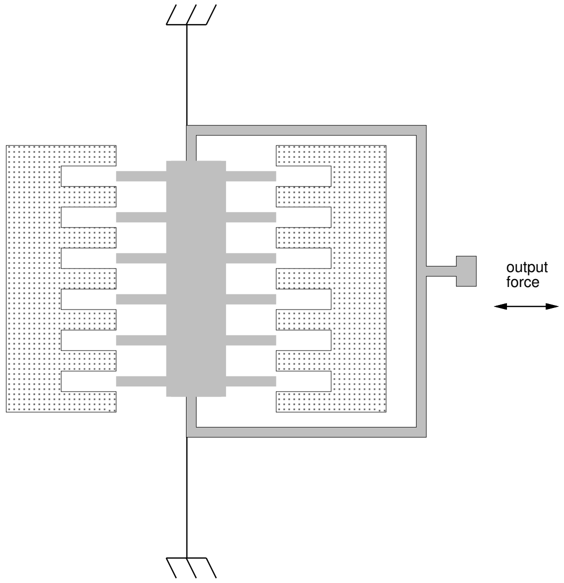

Figure 7: Side drive comb actuator.

where the moving member is attached to the substrate using a suspension. A feature of the side drive comb actuator is that the gaps can be made very small (increasing field strength), and the force is relatively constant over the length of the stroke.

A potential limitation of comb drives is the rather short stroke. Figure 8 shows a planar electrostatic actuator, where a mobile platform is levitated on an air bearing [Pister et al 1990]. The total capacitance seen by the power source is

$$C(x, z) \;=\; C_o + \frac{C_1(z)C_2(x, z)}{C_1(z) + C_2(x, z)}. \tag{9}$$

The tangential force can be calculated as in part b) of the figure assuming that C_1 is constant:

$$F_x(x) \;=\; \frac{1}{2}V^2 \frac{\partial C(x, z)}{\partial x} \;=\; \frac{1}{2}V^2 \epsilon_o \frac{L^2(L + 2x)}{z(L + x)^2}\;, \tag{10}$$

where L is the electrode width. Normalizing by the area orthogonal to the direction of motion, the equivalent pressure is:

$$\frac{F_x(0)}{zL} \;=\; \frac{1}{2}\frac{V^2\epsilon_o}{z^2} \;=\; \frac{1}{2}\epsilon_o |E|^2 \tag{11}$$

as expected. Acceleration is

$$\ddot{x} \;=\; \frac{F_x(0)}{m} \;=\; \frac{1}{2}\frac{V^2\epsilon_o}{zL\delta\rho}\;, \tag{12}$$

where δ is the thickness of the platform and ρ is its density. Note that improved acceleration is possible with gratings on the platform.

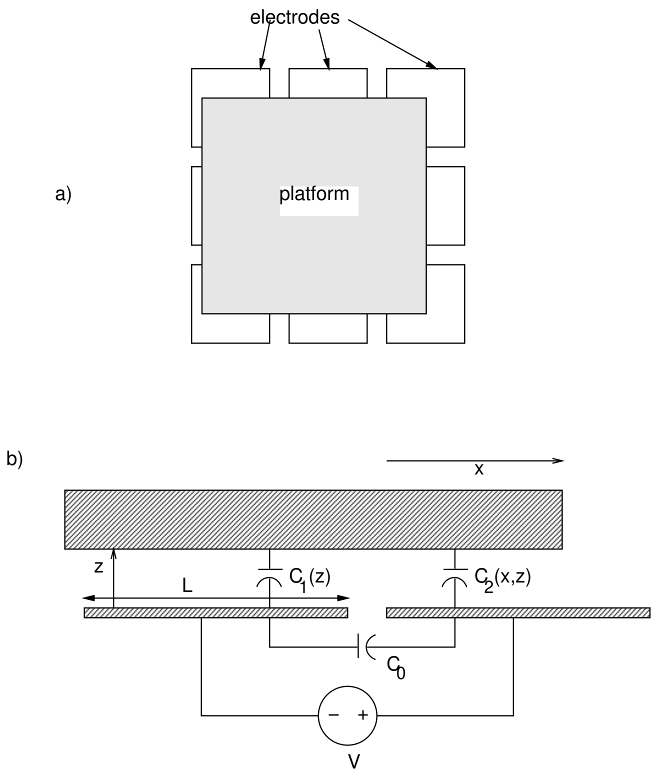

Figure 8: Planar electrostatic drive with levitated platform. a) Electrode configuration. b) Equivalent circuit.

2.1.3 Force Limits for Linear Electrostatic Actuators

It is useful to estimate the maximum force which can be obtained by a linear actuator. As we have seen, the force is proportional to the square of the field strength. With smaller gaps, there are fewer ionizable gas molecules available for breakdown, resulting in higher sustainable field strengths (the Paschen effect). As an indication of the larger fields which are sustainable at smaller dimensions, Figure 9 shows the maximum local field near a charged sphere before breakdown occurs. Experiments have shown that with sub-micron gaps and very smooth surfaces, air will breakdown at fields of $9 \times 10^8 Vm^{-1}$ [Horn and Smith, 1992]. In a vacuum, or with smaller gaps, the absolute limit is set by field emission at $10^9 Vm^{-1}$ for typical materials [Lang et al, 1987]. In practice, thin films such as SiO_2 withstand $2 \times 10^8 Vm^{-1}$ [Fujita and Omodaka, 1987].

Let's estimate the available force from an actuator such as the parallel plate comb drive shown in Figure 5. New surface micromachining techniques such as HEXSIL allow vertical features approaching

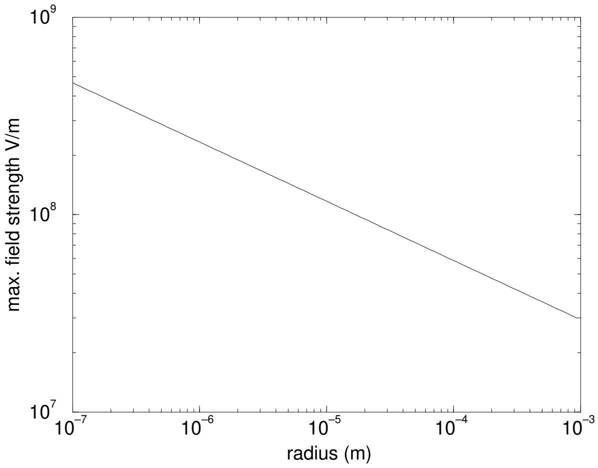

Figure 9: Surface field at breakdown for spheres [Harper, 1967].

$100\mu m$ [Keller and Ferrari, 1994]. Assuming a field of $5 \times 10^7 Vm^{-1}$, with $10\mu m$ per comb, the effective area is $10 cm^2$ giving 10 N force per actual cm^2. This is starting to be enough force to be worthwhile for milli-size robots.

Some representative actuators are summarized in Table 1. In addition to clever mechanical design, such as minimizing contrary forces from suspension springs, the most important limit on peak force is the maximum field strength obtained in practice before breakdown. The maximum field strength is a function of gap size as well as surface roughness.

2.2 Rotary Actuators

A typical rotary side drive motor is shown in Figure 10. These motors are characterized by high rotational speeds (thousands of RPM) and very small torques. By using an offset rotor in the motor (called a wobble or harmonic drive motor), more torque at lower speeds can be obtained, as seen in Figure 11. The equivalent gear ratio is given by:

$$ratio = \frac{d_{inner}}{d_{inner} - d_{outer}}. \tag{13}$$

With typical control of gap sizes, gear ratios up to several hundred have been obtained. Note that the inner rotor is in rolling contact with the outer stator. High field strengths can be used with thin film insulating materials.

Some representative rotary motors are shown in Table 3. Again, the important parameter is the maximum field strength which was actually sustained.

Table 1: Comparison of some representative electrostatic linear actuators. (no load speed).

volume $10^{-9}m^3$	speed s^{-1}	force N	stroke m	power density Wm^{-3}	peak field Vm^{-1}	reference
7×10^4	?	?	3.9×10^{-6}	?	3×10^6	[Fukuda et al 90]
1.2×10^5	100	0.4	4×10^{-4}	200	4×10^5	[Egawa et al 90]
$110 \times 120 \times 2$	10	4.4	0.1	1×10^5	2×10^7	[Niino et al 93]
$70 \times 20 \times 14$	1000	8	240×10^{-6}	2×10^4	2×10^7	[Niino et al 94]
6×10^3	?	70×10^{-6}	9×10^{-6}	?	10^8	[Matsubara et al 91]
400	5000	10^{-7}	6×10^{-6}	200	2×10^7	[Kim et al 92]
$.07 \times .05 \times .5$	50	6×10^{-5}	160×10^{-9}	300	2×10^8	[Akiyama&Fujita 95]

Table 2: Scaling for representative electrostatic linear actuators. (Assuming peak field of $E = 1 \times 10^8 Vm^{-1}$ for $2\mu m$ gap).

Actuator Type	Strain $\frac{m}{m}$	Force N	Stroke m	pressure Nm^{-2}	Energy Density Jm^{-3}
parallel plate	$\leq 90\%$	$\frac{\epsilon_o}{2} L^2 E^2$	z_o	$\frac{\epsilon_o}{2} E^2$	$\frac{\epsilon_o}{2} E^2$
Ideal 1 mm cube	30%	44 mN	0.3 mm	$44 \times 10^3 Nm^{-2}$	$44 \times 10^3 Jm^{-3}$

Table 3: Comparison of Electrostatic Rotary Actuators.

dimensions $r \times h$ (mm)	rot. speed $rads^{-1}$	torque Nm	power density Wm^{-2}	peak field Vm^{-1}	reference.
65×10^{-6}	1500	10^{-11}	4×10^{-3}	10^8	[Mehregany et al 90]
1.6×10^{-3}	?	7×10^{-4}	?	6×10^7	[Trimmer and Jebens, 1989]
05×3	40	2×10^{-7}	900	6×10^7	[Nakamura et al 95]

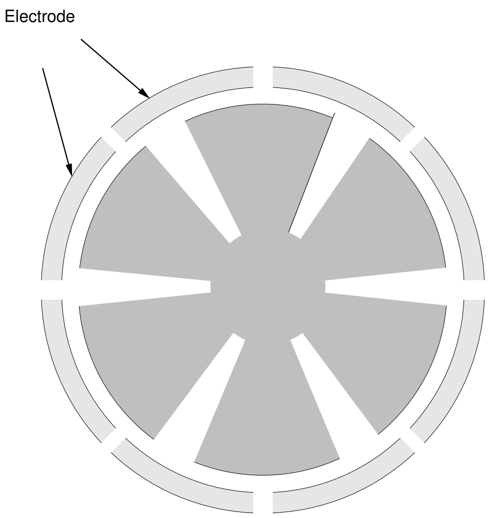

Figure 10: Side drive rotary electrostatic motor.

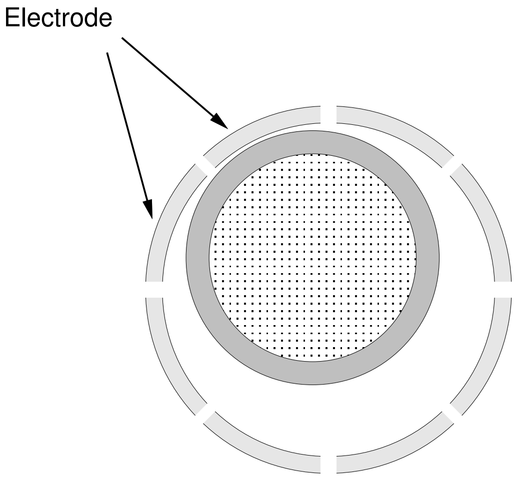

Figure 11: Wobble motor using insulated rotor.

3 Piezoelectric Actuators

Piezoelectric actuators in their normal mode of operation have too short a stroke to be useful for microrobots. However, since the piezoelectric actuator can respond at high frequencies, many small displacements can be added together to give large net motion. In one example, an array of piezoelectrically driven "cilia" can be used to sweep objects along in any direction in the plane (Furuhata et al [1991]). Or transverse surface vibrations can be set up in the surface of a piezo-electric disk which will rotationally displace a disk which is clamped to its top (Raine et al [1993], Udayakumar et al, [1991]). The motor described by Raine et al achieved a torque of 50 nNm at a speed of 20 rad s^{-1}, with a motor diameter of 3.5 mm.

As a piezoelectric element works as both an gener-

Table 4: Properties of common piezoelectrics. From Linvill [1978] and Dario et al [1983]. Notes: (*) breakdown strength rather than polarization limit.

	PVDF	PZT-5H	thin film PZT [Udayakumar et al 1991]
d_{31} $(CN^{-1} = mV^{-1})$	27×10^{-12}	-274×10^{-12}	-88×10^{-12}
d_{33} $(CN^{-1} = mV^{-1})$	31×10^{-12}	593×10^{-12}	220×10^{-12}
stiffness (Nm^{-2})	3.6×10^9	50×10^9	
E_{max} (Vm^{-1})	30×10^6	0.3×10^6	10^8 (*)
permittivity (constant tension)	$12\epsilon_o$	$3400\epsilon_o$	$700\epsilon_o$
density (kgm^{-3})	1.8×10^3	7.5×10^3	
maximum strain $(E_{max} * d_{33})$	1×10^{-3}	2×10^{-4}	
energy density Jm^{-3}	5×10^4	10^3	6×10^5

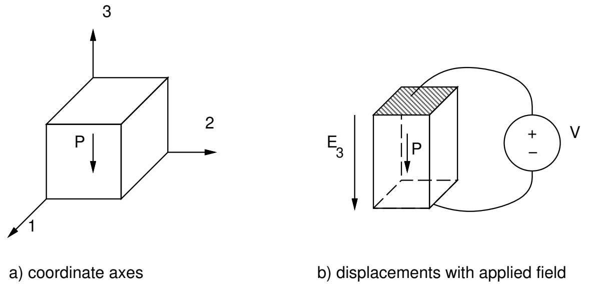

Figure 12: Piezo electric actuator coordinate system.

ator and a motor, there is a coupled set of equations describing charge and strain. In general form [Berlincourt et al 1964], the strain S as a function of applied stress and applied field is:

$$S = s^E T + dE \tag{14}$$

and the charge displacement D is given by:

$$D = dT + \epsilon^T E \ , \tag{15}$$

where S is the strain, s^E is the compliance with electrodes shorted (0 field), T is the applied surface stress, d are the piezo electric constants in strain per applied field, E is the applied field, and ϵ^T is the permittivity at constant stress. For the special case of unclamped sides (stress $T = 0$), and the electric field E_3 applied parallel to the poling direction, the above equations simplify to: $s_3 = E_3 d_{33}$ and $s_1 = E_3 d_{31}$. The maximum field strength which can be applied is limited by depolarization, with a field strength of just $3 \times 10^5 Vm^{-1}$ for PZT. Electrical break down of the piezo electric element is another limitation.

4 Mechanical Transformers

Electrostatic and piezoelectric devices can have large forces with high response frequencies, but small strokes. The small stroke limitations are usually due to the desire to take advantage of greater field strengths at small gaps. Two methods for converting small stroke, high force and high frequency actuation into larger stroke are the inchworm mechanism and traveling mechanical wave mechanisms. The inchworm drive linear actuator of Figure 13 is composed of three linear actuators. Actuators 1 and 3 are simply binary clamps. Actuator 2 is a linear actuator which is controlled longitudinally. By alternately clamping actuators 1 and 3 and extending actuator 2, large effective strokes can be obtained. Note that in principle, the peak force of actuator (assuming no slip) is determined by actuator 2, with no loss in force. The inchworm drive can be used with piezoelectric, electrostatic, or magnetic actuation.

Ultrasonic motors use a piezoelectric element (driven in resonance for higher efficiency) to set up traveling waves (Figure 14). Since points on the surface of the piezo material move elliptically, they drag the slider along with it. While the elliptical motion amplitude is only on the order of nm, the high drive frequencies give relatively high velocities, on the order of cm per second.

One of the classical transformer methods with piezo-electric transducers is the bimorph, made by creating a sandwich of two polarized layers of piezoelectric material (Figure 15). The two types of connection are series [Piezo Systems, 1994]:

$$y = \frac{2L^2}{T} E_3 d_{31} \tag{16}$$

and parallel:

$$y = \frac{4L^2}{T} E_3 d_{31}, \tag{17}$$

with L the length of the cantilever and T the thickness. Significant strokes can be achieved, for example, with

Table 5: Comparison of Piezoelectric Rotary Actuators. (speed at no load, peak torque).

dimensions $\frac{\pi}{4}\phi^2 \times h \times 10^{-9} m^3$	rot. speed $rads^{-1}$	torque Nm	power density Wm^{-3}	peak field Vm^{-1}	reference.
1.5×0.5	30	2×10^{-11}	0.7	10^7	[Udayakumar 91]
30×14	150	10^{-4}	1000	–	[Uchiki 91]
$6 \times 6 \times 2$	60	50×10^{-9}	40	2×10^6	[Racine et al 93]
17×6	70	8×10^{-3}	4×10^5	–	USM-17D [Ueha 93]

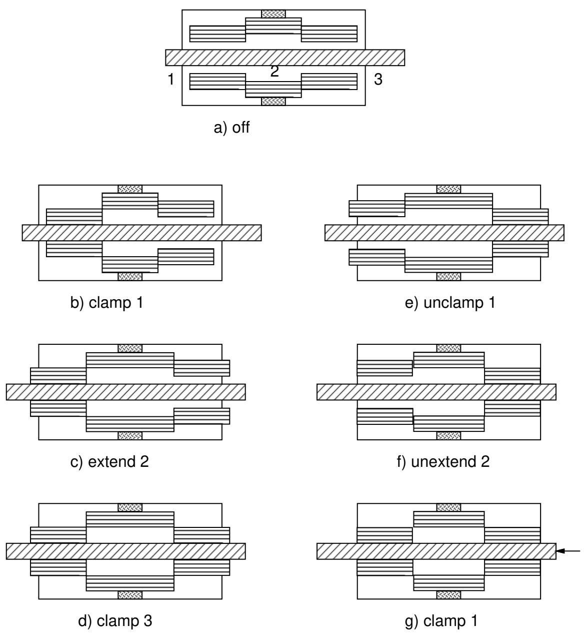

Figure 13: Inchworm drive linear actuator [King et al 1990].

a 25 mm long bimorph one can achieve free deflections of several hundred μm and blocked forces of several hundred mN [Piezo Systems, 1994].

5 Magnetic Field Driven Actuators

Although many of the first micro-actuators have been electrostatic or piezo-electric, electromagnetic actuators have recently received more more attention. One of the particular benefits of electromage-

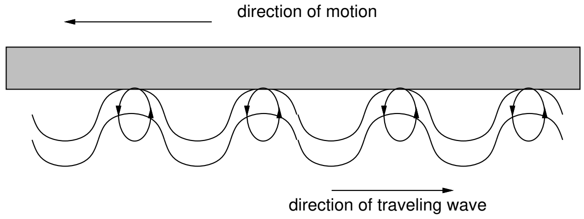

Figure 14: Traveling wave drive. Elliptical motion of contact points in vibrating body applies tangential force to slider.

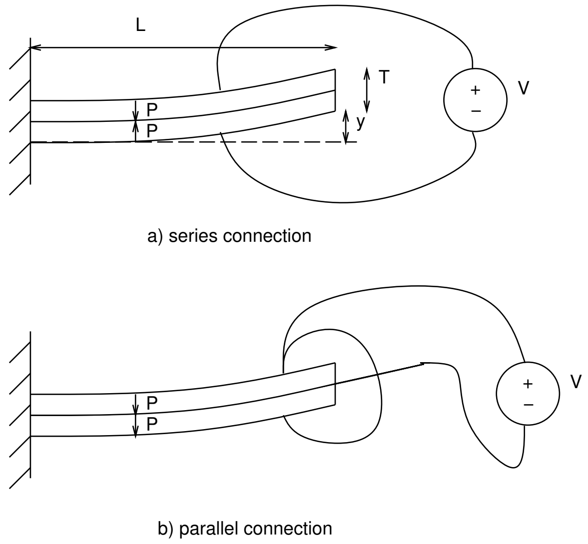

Figure 15: Piezo electric bender.

netic actuation is the comparatively large displacements which can be obtained with moderate force levels. Electrostatic actuation may have problems with charge accumulation in the dielectric if the two charged surfaces make contact, see for example [Anderson and Colgate, 1991]. Another problem is that electrostatic drive won't work in a conductive fluid medium such as water. Magnetic actuation may thus be an attractive alternative, see for example [Busch-Vishniac, 1991]. Magnetics may also be attractive when using an internal high current, low voltage source like a single cell battery, since the coil will usually be fairly low impedance. One of the most significant drawbacks to (non-superconducting) magnetic actuators is the thermal dissipation in coils while maintaining a constant force; in contrast, electrostatic actuators require no power to maintain a constant force with no displacement.

5.1 Linear Electromagnetic Actuators

The simplest magnetic actuator consists simply of a current carrying wire in a constant magnetic field, as shown in Figure 16, with the force per unit current element:

$$d\vec{F} = I d\vec{l} \times \vec{B}. \tag{18}$$

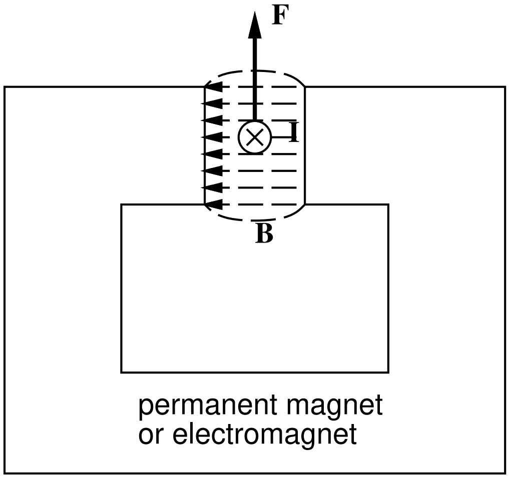

Figure 16: Lorentz force on a wire in constant magnetic field.

Since very strong fixed magnetic fields can be easily provided by miniature permanent magnets, this type of actuator could be attractive for the micro scale. Recently Holzer et al [1995] demonstrated a single turn thin film aluminum coil, with 20 μm displacement, and estimated force of $0.1 \mu N$ using only 20 mA. This compares quite favorably to electrostatic actuator force and stroke. Moving coil type actuators typically use an externally mounted permanent magnet (Figure 17a) while small permanent magnets can be manually placed or deposited on moving structures (Figure 17b).

A 3 DOF actuator was built by attaching a permanent magnet to an elastic suspension above a set of coils (Wagner and Benecke, [1991], Wagner, Kreutzer and Benecke, [1991]). They obtained a deflection of $70 \mu m$ with a force of $450 \mu N$. A linear actuator using superconducting levitation yielded a force of $30 \mu N$ and a 5 mm stroke (Kim, Katsurai, Fujita [1990]). A linear actuator using a self-pressurizing air-bearing gave a peak force of about $2mN$ on a 6.3 mm diameter, 5.0 mm length magnet, with a total travel distance of 20 mm [Fearing, 1992]. (See Figure 18).

A more conventional electromagnetic actuator is shown in Figure 19. This type of device relies more on concentrating the magnetic flux in a narrow gap. The stored magnetic energy in the gap is given by:

$$W = \tfrac{1}{2}\mu_o H^2 = \tfrac{1}{2}\mu_o (\frac{NI}{2})^2 (Az), \qquad (19)$$

where H is the magnetic field, $\mu_o = 4\pi \times 10^{-7} Hm^{-1}$ is the permeability of free space, N is the number of turns, z is the total gap length, and A is the gap area

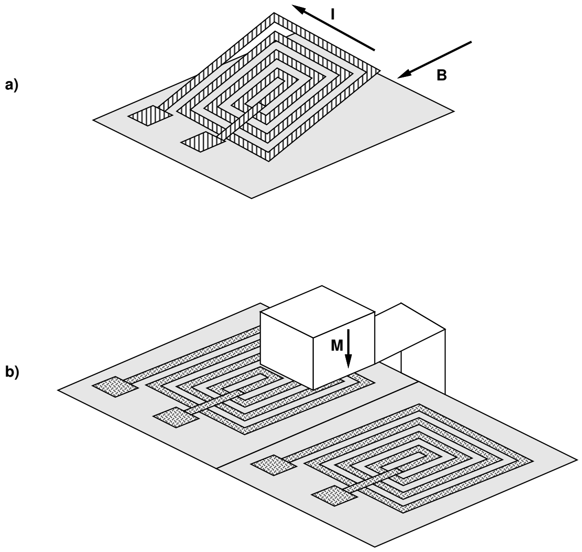

Figure 17: Typical moving coil and moving magnet type Lorentz force actuators.

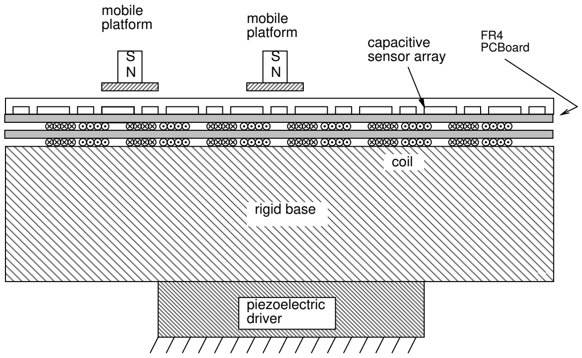

Figure 18: Air bearing levitated planar magnetic actuator.

. The force in the normal direction is given by:

$$F_z(z) = -\frac{\partial W}{\partial z} = \tfrac{1}{2}\mu_o \frac{A}{z^2}(NI)^2. \qquad (20)$$

The equivalent "magnetic pressure" is calculated by the normal force per area or:

$$P_{magnetic} = \tfrac{1}{2}\mu_o (\frac{NI}{z^2})^2. \qquad (21)$$

It is interesting to note that in conventional size machines with flux density on the order of 1 Tesla, pressures of $10^6 Nm^{-2}$ are easily obtained.

A summary of some linear electro-magnetic actuators is shown in Table 6. It is interesting to note that all of the listed actuators except for Ahn and Allen [1993] and Hosaka and Kuwano [1995] use Lorentz type actuation with either moving permanent mag-

Table 6: Comparison of some representative linear magnetic actuators. (Stroke at no load, peak force).

dimensions $10^{-9}m^3$	speed s^{-1}	force N	stroke m	power density Wm^{-3}	current amp-turns	peak field Am^{-1}	reference
$0.2 \times .02 \times .004$	10^4	10^{-9}	2×10^{-8}	10	1	-	[Yanagisawa 91]
$0.3 \times 0.3 \times 2$	2500	10^{-7}	5×10^{-5}	100	.02	-	[Holzer et al 95]
$0.4 \times 0.4 \times 0.5$	1000	2.9×10^{-6}	10^{-4}	3000	0.12	10^5	[Liu et al 94]
$1.6 \times 1.4 \times 2.4$	50	1.3×10^{-4}	9×10^{-4}	1000	1.95	400	[Wagner et al 93]
$1 \times 1 \times 0.5$	-	10^{-4}	10^{-3}	-	-	2×10^4	[Liu et al 1995]
$2 \times 2 \times 0.3$	-	8×10^{-7}	8×10^{-6}	-	0.9	6×10^5	[Ahn & Allen 93]
$3 \times 3 \times 3$	10	10^{-3}	5×10^{-4}	200	1	-	[Robichaux 92]
$2 \times 2 \times 2$	600	2×10^{-4}	2.2×10^{-4}	3000	6	-	[Tabat et al 97]
$7 \times 2 \times 2$	-	1.5×10^{-2}	4×10^{-4}	-	50	-	[Hosaka 95]
$1 \times 7 \times 7$	200	3×10^{-4}	1×10^{-5}	10	3	-	[Wagner et al 91]
$5 \times 5 \times 3$	3	2×10^{-6}	2.5×10^{-3}	0.2	.65	-	[Maeda et al 93]
$10 \times 10 \times 3$	5	4×10^{-3}	6.6×10^{-3}	400	16	1000	[Fearing 95]
$4 \times 6 \times 0.6$	300	1×10^{-3}	300×10^{-6}	6000	50	-	[Guckel et al 96]
2×10^5	30	1.2	3×10^{-3}	500	-	-	[Salcudean Yan 94]
$\pi(15)^2 \times 20$	.5	0.9	20×10^{-3}	4	-	8000	[Iizuka&Fujita 96]
$\pi(6.4)^2 \times 13$	600	0.35	5×10^{-4}		6.5×10^4	-	BEI Voice coil

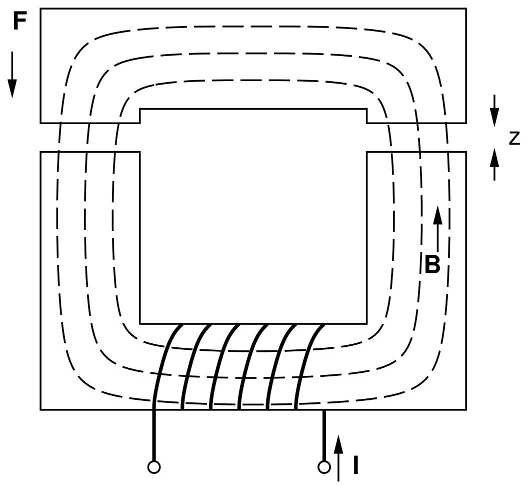

Figure 19: Electromagnetic actuator.

net or moving coil. The two exceptions use permeable materials for the magnetic circuit and an air gap.

5.2 Rotary Electromagnetic Actuators

Recently, electromagnetic motors have been fabricated using lithographic and thick film techniques (Ahn et al [1993], Guckel et al [1993]). The motor of Ahn et al has a predicted torque of $1.2\mu Nm$ with a motor diameter of 1.5 mm.

Conventional electromagnetic motors are also shrinking in size. An electric motor was built into the 4.6 mm car designed by Hisanaga et al [1991].

5.3 Magnetostrictive Devices

There are also analogs to the piezoelectric effect for magnetic materials. One advantage of the magnetic field actuation is the comparatively long range which is good for tetherless drive, such as the milli-robot described in Fukuda et al [1991].

6 Power Limits

To determine an upper bound on achievable power delivery to a load, consider an actuator which provides constant force with respect to position such as the tangential electrostatic drive given in Eqn. 8. The maximum power will be delivered to the load when the load impedance is equal to the source impedance. In the simplest case, the source impedance is just the inherent viscous damping of the actuator b. Thus with source plus load impedance equal to $2b$, the final velocity is $\frac{F}{2b}$, and the power delivered to the load impedance is just

$$P = \frac{F^2}{4b} \quad . \tag{22}$$

As a crude approximation to the drag force, assuming only viscous drag between a sliding horizontal plate as in Figure 20, the drag force is:

$$F_{drag} = \frac{\mu_{air} l^2}{z} \dot{x} = b\dot{x} \tag{23}$$

where $\mu_{air} = 1.8 \times 10^{-5} Nsm^{-2}$ is the viscosity of air at room temperature, and l is the length of the side of a slider. A more accurate viscous damping model is discussed in Cho et al [1993].

Substituting in the expression for the force (eqn. 8), and assuming an air gap $z = 2\mu m$ and electric field strength $2 \times 10^7 Vm^{-1}$, we obtain power of:

$$P = \frac{{\epsilon_o}^2 n^2 V_o^4}{16\mu_{air} z} = 350 \times 10^{-9} W \tag{24}$$

Table 7: Comparison of some representative rotary magnetic actuators. (speed at no load, peak torque).

dimensions $r \times h(mm)$	speed $rads^{-1}$	torque Nm	efficiency %	power density Wm^{-3}	current amp-turns	peak field Am^{-1}	reference
6×1.5	200	1×10^{-7}	$< 10^{-4}$	500	2.5	90	[Wagner et al 93]
3×0.5	1200	10^{-9}	10^{-6}	300	10	?	[Guckel et al 1993]
1.5×0.5	50	10^{-6}	$> 10^{-4}$	5×10^4	20	6×10^5	[Ahn et al 93]
$2 \times 3.7 \times 0.5$	150	10^{-6}	.002	3×10^3	20	?	[Teshigaraha 95]
10×2.5	20	350×10^{-6}	8	3×10^4	15	?	[Stefanini et al 96]
2.8×5	1200	10^{-6}	.002	10^4	?	?	Seiko E-HM0305
$.95 \times 5.5$	10^4	7.5×10^{-6}	50?	1.2×10^6	?	?	Faulhaber BL 1900
1.5×8.32	10^4	3×10^{-5}	> 90	2×10^6	?	?	RMB Smoovy SYV30001
2.5×13	10^4	150×10^{-6}	> 90	1.3×10^6	?	?	RMB Smoovy SYVP50002
19×62	700	4×10^{-2}	75	4×10^5	?	?	Dynetic MS1509
17×57	1500	0.1	76	3×10^6	210	?	Astroflight 603
12×43	1500	4.6×10^{-2}	80	4.5×10^6	100	?	Astroflight 802

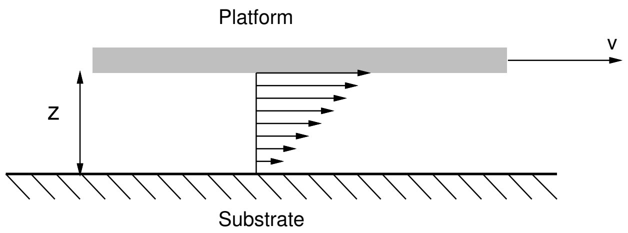

Figure 20: Drag force on slider.

where $V_o = 40V$, and n is the number of electrodes. For a film actuator $100\mu m$ thick with $100\mu m$ wide electrodes, the power density is independent of size, and is shown in Figure 21.

7 Summary

The performance of electrostatic and magnetic actuators can best be compared by considering idealized actuators for each case of the same dimension, for example, a 1 mm cube. While maximum pressure and strain are easy to estimate, the maximum frequency response while be strongly dependent on the actuator's stiffness, mass, and internal damping, and hence strongly dependent on construction techniques. For example, a vacuum gap electrostatic actuator could have significantly higher frequency response than an air gap actuator. Table 8 compares best case assumptions for the various actuator technologies. It is interesting to compare various micro-actuators with each other and with estimated physical limits. Figure 21 summarizes the actuators detailed in the previous tables for which data is available to calculate a power density. The general trend is towards lower power density for the smallest actuators. The main reason for lower power density is the comparatively large supporting structure, typically the thickness of a silicon wafer (0.5mm). A significant improvement could be obtained simply by reducing the excess supporting structure volume.

While there is currently much research activity in micro-actuators, there are very few off-the-shelf actuators available in the millimeter size region. Hopefully the demand for actuators for micro-robotic applications will stimulate their further development.

Acknowledgments

I would like to thank H. Furuichi, E. Tan, and B. Gray for helpful discussions, and J. Judy for making his bibliography available.

References

[1] C.H. Ahn, Y.J. Kim, and M.G. Allen, "A Planar Variable Reluctance Magnetic Micromotor with Fully Integrated Stator and Wrapped Coils" *Proc. IEEE Micro Electro Mechanical Systems*, pp. 1-6, Fort Lauderdale, FL Feb. 7-10, 1993.

[2] C.H Ahn and M.G. Allen, "A Fully Integrated Surface Micromachined Magnetic Actuator with a Multilevel Meander Magnetic Core", *Jnl. of Microelectromechanical Systems*,vol. 2, no. 1, pp. 15-22, March 1993.

[3] T. Akiyama and H. Fujita, "A Quantitative Analysis of Scratch Drive Actuator using Buckling Motion", *Proc. IEEE Micro Electro Mechanical Systems* , pp. 310-315, Amsterdam Jan. 29-Feb 2, 1995.

[4] K. M. Anderson and J. Edward Colgate, "A model of the attachment/detachment cycle of electrostatic micro actuators", *ASME Micromechanical Sensors, Actuators, and Systems*, DSC-vol. 32, pp. 255-268, Atlanta, GA Dec. 1-6, 1991.

[5] D.A. Berlincourt, D.R. Curran, and H. Jaffe, "Piezoelectric and Piezomagnetic Materials and Their Function in Transducers', in *Physical Acoustics: Principles and Methods* edited by W.P Mason, New York: Academic Press 1964.

[6] S.M. Bobbio, M.D. Kellam, B.W. Dudley, S. Goodwin-Johansson, S.K. Jones, J.D. Jacobson, F.M. Tranjan, and T.D. DuBois, "Integrated Force Arrays", *Proc. IEEE Micro Electro Mechanical Systems* , pp. 149-154, Fort Lauderdale, FL Feb. 7-10, 1993.

[7] B. Bollee, "Electrostatic Motors", *Philips Technical Review* , vol. 30, no. 6/7, pp. 178-194, 1969.

[8] I.J. Busch-Vishniac, "The Case for Magnetically Driven Micro-Actuators", *ASME Micromechanical Sensors, Actuators, and Systems*,DSC-vol. 32, pp. 287-302, Atlanta, GA Dec. 1-6, 1991

Table 8: Scaling for representative linear actuators. (Frequency is calculated for 1 mm cube actuator).

Actuator Type	Strain $\frac{m}{m}$	Frequency $\frac{m}{m\,s}$	Pressure Nm^{-2}	Power Density $Jm^{-3}s^{-1}$	Assumptions
electrostatic	30%	5000?	4×10^4	10^4	$E = 1 \times 10^8 Vm^{-1}$
PZT	2×10^{-4}	10^6	10^3	2×10^5	$E = 3 \times 10^5 Vm^{-1}$

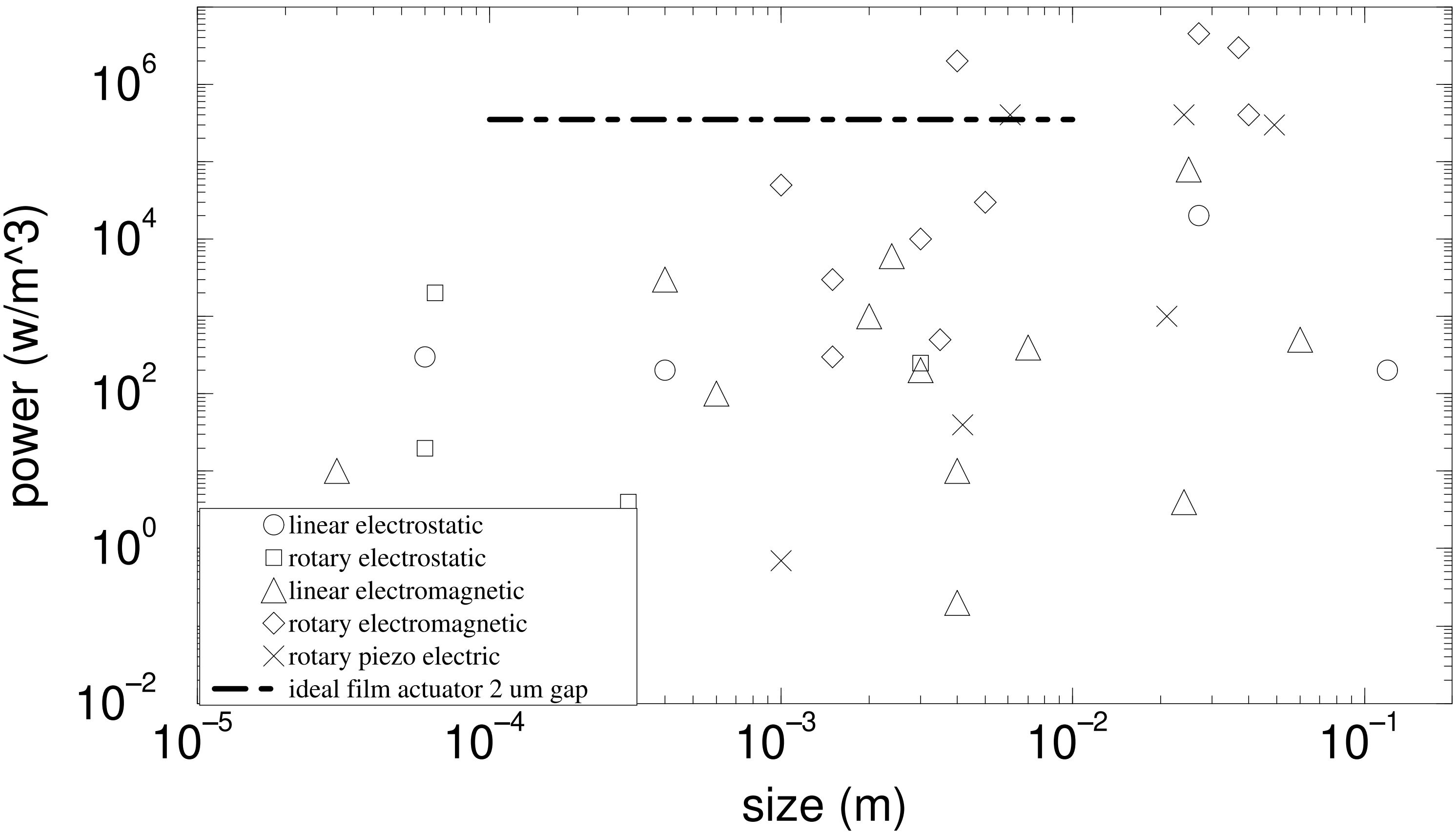

Figure 21: Comparison of implemented micro-actuators. Power is calculated as an upper bound using $force \times \frac{stroke}{sec}$. Volume includes substrate thickness. Only points are shown for which experimental data exists. The dot-dash line shows a calculated bound for a 100 μm thick film actuator with 2 μm air gap assuming laminar air drag forces.

[9] Y-H. Cho, B.M. Kwak, A.P. Pisano, and R.T. Howe, "Viscous Energy Dissipation in Laterally Oscillating Planar Microstructures: A Theoretical and Experimental Study", *Proc. IEEE Micro Electro Mechanical Systems,* pp. 93-98, Fort Lauderdale, FL, Feb 7-10, 1993.

[10] J.E. Colgate, H. Matsumoto and W. Wannasuphoprasit, "Linear Electrostatic Actuators: Gap Maintenance via Fluid Bearings", *Robotics and Computer-Intergated Manufacturing,* vol. 10, no. 5, pp. 365-376, 1993.

[11] M.J. Daneman, N.C. Tien, O. Solgaard, A.P. Pisano, K.Y. Lau, and R.S. Muller, "Linear Microvibromotor for Positioning Optical Components", *Jnl. of Microelectromechanical Systems,* , vol. 5, no.3 , pp. 159-165, Sept. 1996.

[12] P. Dario, R. Valleggi, M.C. Carrozza, M.C. Montesi, and M. Cocco, "Microactuators for microrobots: a critical survey", *J. Micromech. Microeng.* vol. 2, pp. 141-157, 1992.

[13] P. Dario, C. Domenici, R. Bardelli, D. DeRossi, and P.C. Pinotti, "Piezoelectric Polymers: New Sensor Materials for Robotic Applications", *13th Int. Symp. Industrial Robots,*pp. 14:34-49, Chicago IL April 19-20, 1983.

[14] S. Egawa and T. Higuchi, "Multi-layered electrostatic film actuator", *Proc. of the IEEE Workshop on Micro-Electro Mechanical Systems* , pp. 166-171, Napa Valley, CA Feb. 11-14, 1990.

[15] S. Egawa,, T. Niino, and T. Higuchi, "Film Actuators:Planar, Electrostatic Surface-Drive Actuators", *IEEE Micro Electro Mechanical Systems",* pp. 9-14, Nara, Japan, Feb. 1991

[16] L.S. Fan, Y.C. Tai, and R.S. Muller, "Integrated Movable Micromechanical Structures for Sensors and Actuators," *IEEE Transactions on Electron Devices* ED-35, pp. 724-773 June 1988.

[17] R.S. Fearing, "A Miniature Mobile Platform on an Air Bearing", *Third Int. Symp. on Micro Machine and Human Sciences*, Oct. 14-16, 1992, Nagoya, Japan.

[18] G. Fuhr, R. Hagedorn and J. Gimsa, "Analysis of the torque-frequency characteristics of dielectric induction motors", *Sensors and Actuators A*, vol. 33, pp. 237-247, 1992.

[19] G. Fuhr, R. Hagedorn, T. Muller, W. Benecke, U. Schnakenberg and B. Wagner, "Dielectric Induction micromotors: field levitation and torque-frequency characteristics", *Sensors and Actuators A*, vol. 33, pp. 525-530, 1992.

[20] H. Fujita and A. Omodaka, "Electrostatic Actuators for Micromechatronics", *IEEE MicroRobots and Teleoperators Workshop,* Hyannis, MA Nov. 9-11, 1987.

[21] H. Fujita and Kaigham J. Gabriel, "New Opportunities for MicroActuators", 1991 Int. Conf. on Solid-State Sensors and Actuators (Transducers '91) June 1991, San Francisco, CA, pp. 14-20.

[22] T. Fukuda and T. Tanaka, "Micro-Electro Static Actuator with Three Degrees of Freedom", *Proc. of the IEEE Workshop on Micro-Electro Mechanical Systems* , Napa Valley, CA Feb. 11-14, 1990.

[23] T. Fukuda, H. Hosokai, H. Ohyama, H. Hashimoto and F. Arai, "Giant Magnetostrictive Alloy (GMA) Applications to Micro-Mobile Robot as a Micro Actuator without Power Supply Cables", *IEEE Micro Electro Mechanical Systems",* pp. 210-215, Nara, Japan, Feb. 1991.

[24] T. Furuhata, T. Hirano, and H. Fujita, "Array-Driven Ultrasonic Microactuators- arrayed microactuator modules that have swing pins", 1991 Int. Conf. on Solid-State Sensors and Actuators (Transducers '91), June 1991, San Francisco, CA, pp. 1056-1059.

[25] T. Furuhata, T. Hirano, L.H. Lane, R.E. Fontana, L.S. Fan, H. Fujita, "Outer Rotor Surface Micromachined Wobble Micromotor", *Proc. IEEE Micro Electro Mechanical Systems*, pp. 161-166. Fort Lauderdale, FL Feb. 7-10, 1993.

[26] E.J. Garcia and J.J. Sniegowski, "The Design and Modelling of a Comb-Drive-Based Microengine for Mechanism Drive Applications", 7th Int. Conf on Solid-State Sensors and Actuators (Transducers '93), pp. 763-766, Yokohama, Japan, June 1993.

[27] H. Guckel, T. Earles, J. Klein, J.D. Zook, and T. Ohnstein, "Electromagnetic Linear actuators with inductive position sensing", *Sensors and Actuators* , vol. A53, pp. 386-391, 1996.

[28] H. Guckel, T.R. Christenson, K.J. Skrobis, T.S. Jung, J. Klein, K.V. Hartojo, and I. Widjaja, "A First Functional Current Excited Planar Rotational Magnetic Micromotor", *Proc. IEEE Micro Electro Mechanical Systems*, pp. 7-11, Fort Lauderdale, FL Feb. 7-10, 1993.

[29] B. Hannaford, P.-H. Marbot, P. Buttolo, M. Moreyra, S. Venema, "Scaling of Direct Drive Robot Arms", *Int. Jnl. of Robotics Research* , vol. 15, no. 5, pp. 459-472, Oct. 1996

[30] B. Hannaford and J. Winters, "Actuator Properties and Movement Control: Biological and Technological Models", in *Multiple Muscle Systems: Biomechanics and Movement Organization* , edited by J.M. Winters and S. L.-Y. Woo, pp. 101-120, New York: Springer-Verlag 1990.

[31] M. Hisanaga, T. Kurahashi, M. Kodera, and T. Hattori, "Fabrication of a 4.8 Millimeter Long Microcar", Proc. Second Int. Symp. on Micro Machine and Human Science, pp. 43-46, Nagoya, Japan, Oct. 8-9, 1991.

[32] W.R. Harper, *Contact and frictional electrification*, Oxford: Clarendon Press, 1967.

[33] J.W. Hollerbach, I.W. Hunter, and J. Ballantyne, "A Comparative Analysis of Actuator Technologies for Robotics", in *The Robotics Review 2* , edited by O. Khatib, J.J. Craig, and T. Lozano-Perez, pp. 299-342, Cambridge: MIT Press, 1992.

[34] R. Holzer, I. Shimoyama, and H. Miura, "Lorentz Force Actuation of Flexible Thin-Film Aluminum Microstructures", *Proc. IEEE-RSJ Intelligent Robots and Systems,*pp. 156-161, Pittsburgh, PA August 3-5, 1995.

[35] R.G. Horn, D.T. Smith, "Contact electrification and adhesion between dissimilar materials." *Science*, 17 April 1992, vol.256, (no.5055):362-4.

[36] H. Hosaka and H. Kuwano, "Design and Fabrication of Miniature Relay Matrix and Investigation of Electromechanical Interference in Multi-Actuator Systems", *Proc. IEEE Micro Electro Mechanical Systems* , pp. 313-318, Amsterdam Jan. 29-Feb 2, 1995.

[37] I.W. Hunter and S. Lafontaine, "A Comparison of Muscle with Artificial Actuators", Solid-State Sensor and Actuator Workshop, pp. 178-185, Hilton Head, SC, June 22-25, 1992.

[38] T. Iizuka and H. Fujita, "A Threaded Wobble Motor with a 6-pole Stator", *7th Int. Symp. on Micro Machine and Human Science* , pp. 189-193, Nagoya, Japan, Oct. 1997.

[39] T. Inoue, K. Iwatani, I. Shimoyama and H. Miura, "Micromanipulation Using Magnetic Field", *IEEE Int. Conf. Robotics and Automation* , pp. 679-684, Nagoya, Japan May 1995.

[40] H. Ishihara, F. Arai, and T. Fukuda, "Micro Mechatronics and Micro Actuators", *IEEE/ASME Trans. on Mechatronics,* vol. 1, no. 1, pp. 68-79, March 1996.

[41] J.D. Jacobson, S.H. Goodwin-Johansson, S.M. Bobbio, C.A. Bartlett, and L.N. Yadon, "Integrated Force Arrays: Theory and Modelling of Static Operation", *Jnl. of Microelectromechanical Systems,*vol. 4, no. 3, pp. 139-150, Sept. 1995

[42] J.W. Judy, R.S. Muller, and H.H. Zappe, "Magnetic Microactuation of Polysilion Flexure Structures", *IEEE Solid-State Sensor and Actuator Workshop* Solid-State Sensor and Actuator Workshop, Hilton Head South Carolina,pp. 43-48, 1994.

[43] C. Keller and M. Ferrari, "Milli-Scale Polysilicon Structures", *IEEE Solid-State Sensor and Actuator Workshop* Solid-State Sensor and Actuator Workshop, Hilton Head, South Carolina, pp. 132-137, 1994.

[44] C-J. Kim, A.P. Pisano, and R.S. Muller, "Silicon-processed overhanging microgripper", *Jnl. of Microelectromechanical Systems*, pp. 31-36, vol. 1, no. 1, March 1992.

[45] Y. Kim, M. Katsurai, and H. Fujita, "Fabrication and Testing of a Micro Superconducting Actuator using the Meissner Effect", *Proc. IEEE Micro Electro Mechanical Systems*, pp. 61-66, Napa Valley, CA, Feb. 1990.

[46] T.G. King, M.E. Preston, B.J.M. Murphy, D.S. Cannell, "Piezoelectric ceramic actuators: a review of machinery applications", *Precision Engineering* , vol. 12, no. 3, pp. 131-136, 1990.

[47] R.D. Kornbluh, G.B. Andeen, and J.S. Eckerle, "Artificial Muscle: The next generation of robotic actuators", *4th World Conf. on Robotics Research,* Sept. 17-19, 1991, Pittsburgh, PA.

[48] P. Krulevitch, A.P. Lee, P.B. Ramsey, J.C. Trevino, J. Hamilton, and M.A. Northrup, "Thin Film Shape Memory Allor Actuators", *Jnl. of Microelectromechanical Systems* , vol. 5, no. 4, pp. 270-282, Dec. 1996.

[49] J.H. Lang, M.A. Schlecht and R.T. Howe, "Electric Micromotors: Electromechanical Characteristics", *IEEE MicroRobots and Teleoperators Workshop,* Hyannis, MA Nov. 9-11, 1987.

[50] A.P. Lee and A.P. Pisano, "An Impact-Actuated Micro Angular Oscillator–Design, Testing and Dynamic Analysis", ASME Micromechanical Sensors, Actuators, and Systems, DSC-vol. 32, Atlanta, GA Dec. 1-6, 1991.

[51] J.G. Linvill, "PVF2- Models, Measurements and Device Ideas", Stanford University, Integrated Circuits Lab Technical Report #4843-2.

[52] C. Liu, T. Tsao, Y.-C. Tai, and C-M. Ho, "Surface Micromachined Magnetic Actuators" *IEEE Micro Electro Mechanical Systems* , pp. 57-62, Oiso, Japan, Jan. 25-28, 1994.

[53] C. Liu, T. Tsao, and Y.-C. Tai, "Out of Plane Permalloy Magnetic Actuators for Delta-Wing Control", *Proc. IEEE Micro Electro Mechanical Systems,* pp. 7-12, Amsterdam Jan. 29-Feb 2, 1995.

[54] T. Matsubara, M. Yamaguchi, K. Minami, and M. Esashi, "Stepping Electrostatic Microactuator", 1991 Int. Conf. on Solid-State Sensors and Actuators (Transducers '91), June 1991, San Francisco, CA, pp. 50-53.

[55] Y. Maeda, K. Aihara, and H. Fujita, "A Vacuum-compatible X-Y micro-actuator using the levitational effect of a superconductor" *Robotics, Mechatronics and Manufacturing Systems",* ed. by T. Takamori and K. Tsuchiya, North-Holland Elsevier 1993, pp. 509-514.

[56] M. Mehregany, P. Nagarkar, S.D. Senturia, and J.H. Lang, "Operation of Microfabricated Harmonic and Ordinary Side-Drive Motors", *Proc. IEEE Micro Electro Mechanical Systems*, pp. 1-8, Napa Valley, CA, Feb. 1990.

[57] K. Nakamura, H. Ogara, S. Maeda, U. Sangawa, S. Aoki and T. Sato, "Evaluation of the Micro Wobble Motor Fabricated by Concentric Buildup Process", *Proc. IEEE MEMS,* pp. 374-379, Amsterdam Jan. 29-Feb 2, 1995.

[58] M. Nakasuji and, H. Shimizu, "Low voltage and high speed operating electrostatic wafer chuck." *Journal of Vacuum Science & Technology A (Vacuum, Surfaces, and Films),* Nov.-Dec. 1992, vol.10, (no.6):3573-8.

[59] B.W. Niebel, A.B. Draper, R.A. Wysk, *Modern Manufacturing Process Engineering,* New York: McGraw-Hill, 1989.

[60] T. Niino, S. Egawa, and T. Higuchi, "High-Power and High-Efficiency Electrostatic Actuator" *Proc. IEEE Micro Electro Mechanical Systems* , pp. 236-241, Fort Lauderdale, FL Feb. 7-10, 1993.

[61] T. Niino, S. Egawa, H. Kimura, and T. Higuchi, "Electrostatic Artificial Muscle: Compact High-Power Linear Actuators with Multiple-Layer Structures", *IEEE Micro Electro Mechanical Systems* , pp. 130-135, Oiso, Japan, Jan. 25-28, 1994.

[62] Piezo Systems, Inc. "Piezoceramic Application Data", Cambridge, MA 1994.

[63] K.S.J. Pister, M.W. Judy, S.R. Burgett, and R.S. Fearing, "Microfabricated Hinges", *Sensors and Actuators A* , vol. 33, pp. 249-256, 1992.

[64] R.H. Price, J.E. Wood, and S.C. Jacobsen, "Modelling Considerations for Electrostatic Forces in Electrostatic Microactuators", *Sensors and Actuators* , vol. 20, pp. 107-114, 1989.

[65] G.-A. Racine, R. Luthier, and N.F. de Rooij, "Hybrid Ultrasonic Micromachined Motors" *Proc. IEEE Micro Electro Mechanical Systems* , pp. 128-132. Fort Lauderdale, FL Feb. 7-10, 1993.

[66] J. Robichaux and S. Ahmed, "Magnetically Levitated Micro-Robots: Design, Control, Experimentation and Applications", *Robotics and Manufacturing recent trends in reseearch, education, and applications, Proc. of the 4th Int. Symp. on Robotics and Manufacturing,*Nov. 11-13, 1992, Sante Fe NM pp. 9-14.

[67] H. Saeki, T. Tanaka, T. Fukuda, K. Kudou, et al "New electrostatic micromanipulator which dislodges adhered dust particles in vacuum". *Journal of Vacuum Science & Technology B (Microelectronics Processing and Phenomena),* Nov.-Dec. 1992, vol.10, (no.6):2491-2.

[68] S. E. Salcudean and J. Yan, "Towards a Force Reflecting Motion-scaling system for Microsurgery", *IEEE Int. Conf. on Robotics and Automation*, pp. 2296-2301, San Diego, CA, May 8-13, 1994

[69] I. Shimoyama, "Scaling in Microrobots", *Proc. IEEE/RSJ Intelligent Robots and Systems*, pp. 208-211, Pittsburgh, PA August 3-5, 1995.

[70] C. Stefanini, M.C. Carroza and P. Dario, "A Mobile Microrobot Driven by a New Type of Electromagnetic Micromotor", Seventh Int. Symp. on Micro Machine and Human Science, Nagoya, Japan, Oct. 1996.

[71] K. Suzuki, H. Miura, I. Shimoyama and Y. Ezura, "Creation of an Insect-based Microrobot with an External Skeleton and Elastic Joints", *Proc. IEEE Micro Electro Mechanical Systems Workshop,* Travemunde, Germany, February 4-7, 1992, pp. 190-195.

[72] N. Tabat, J. Klein, and H, Guckel, "Single Flux-Path Bidirectional Linear Actuator", *Transducers '97: Int. Conf. on Solid-State Sensors and Actuators,* pp. 789-792, Chicago, June 16-19, 1997.

[73] Y-C. Tai, L-S. Fan, and R.S. Muller, "IC Processed Micromotors: Design, Technology, and Testing", IEEE Solid State Sensor and Actuator Workshop, pp. 1-6, Hilton Head, South Carolina, 1989.

[74] A. Teshigahara, M. Watanabe, N. Kawahara, Y. Ohtsuka, and T. Hattori, "Performance of a 7 mm Microfabricated Car", *IEEE Jnl. of Microelectromechanical Systems,* vol. 4, no. 2, pp. 76-80, June 1995.

[75] W.S.N. Trimmer and K.J. Gabriel, "Design Considerations for a Practical Electrostatic Micro-Motor," *Sensors and Actuators,* vol. 11, pp. 189-206, 1987.

[76] W. Trimmer and R. Jebens, "Actuators for Micro Robots", *IEEE Int. Conf. on Robotics and Automation,* Scottsdale, AZ, May 1989, pp. 1547-1552.

[77] W. Trimmer and R. Jebens, "An Operational Harmonic Electrostatic Motor", *IEEE Micro Electro Mechanical Systems Workshop* , pp. 13-16, 1989.

[78] T. Uchiki, T. Nakazawa, K. Nakamura, M. Kurosawa, and S. Ueha, "Ultrasonic Motor Utilizing Elastic Fin Rotor", *1991 Ultrasonics Symposium,* pp. 929-932, Dec. 8-11, Lake Buena Vista, Florida.

[79] K.R. Udayakumar, S.F. Bart, A.M. Flynn, J. Chen, L.S. Tavrow, L.E. Cross, R.A. Brooks, and D.J. Ehrlich, "Ferroelectric Thin Film Ultrasonic Micromotors", *IEEE Micro Electro Mechanical Systems"* , pp. 109-113, Nara, Japan, Feb. 1991

[80] S. Ueha and Y. Tomikawa, *Ultrasonic motors : theory and applications* Oxford : Clarendon Press ; New York : Oxford University Press, 1993.

[81] B. Wagner and W. Benecke, "Microfabricated Actuator with Moving Permanent Magnet", *Proc. IEEE Micro Electro Mechanical Systems,* pp. 27-32, Nara, Japan, Feb. 1991.

[82] B. Wagner, M. Kreutzer, and W. Benecke, "Electromagnetic MicroActuators with Multiple Degrees of Freedom" *1991 Int. Conf. on Solid-State Sensors and Actuators (Transducers '91),* June 1991, San Francisco, CA, pp. 614-617.

[83] B. Wagner, M. Kreutzer, and W. Benecke, "Permanent Magnet Micromotors on Silicon Substrates", *Jnl. of Microelectromechanical Systems,* vol. 2, no. 1, pp. 23-29, 1993.

[84] B. Wagner, G. Fuhr, T. Muller, T. Schnelle and W. Benecke, "Fluid-filled dielectric Induction Micromotor with Al-SiO2 Rotor" *Proc. IEEE Micro Electro Mechanical Systems,* pp. 139-142, Fort Lauderdale, FL Feb. 7-10, 1993

[85] J.E. Wood, S.C. Jacobsen, and K.W. Grace, "SCOFFS: A small Cantilevered Optical Fiber Servo System", *IEEE Micro-Robots and Teleoperators Workshop,* Hyannis, MA Nov. 9-11, 1987.

[86] M. Yamaguchi, S. Kawamura, K. Minami, and M. Esashi, "Distributed Electrostatic Micro Actuator" *Proc. IEEE Micro Electro Mechanical Systems* , pp. 18-23, Fort Lauderdale, FL Feb. 7-10, 1993.

[87] K. Yanagisawa, A. Tago, T. Ohkubo, and H. Kuwano, "Magnetic Micro-Actuator", *Proc. IEEE Micro Electro Mechanical Systems,* pp. 120-124, Nara, Japan, Feb. 1991.

[88] R. Yeh, E.J. Kruglick, M. Klitzke, and K.S.J. Pister, "Towards an Articulated Silicon Microrobot" Winter Annual Meeting, ASME, Dec. 1994.